

17.4 Evaluation of the Relationship between NSSL MRMS Rotational Tracks and Tornadoes in Iowa

Raymond A. Wolf*

NOAA/National Weather Service, Davenport Iowa

Gregory J. Stumpf

Cooperative Institute for Mesoscale Meteorology Studies, University Of Oklahoma, Norman, Oklahoma
NOAA/National Severe Storms Laboratory, Norman, Oklahoma

1. INTRODUCTION

Quantitative evaluation of rotational shear is a common technique used by National Weather Service (NWS) meteorologists interrogating WSR-88D data to determine the strength of mesocyclones in supercells or mesovortices in quasi-linear convective systems (QLCSs) where tornadoes are considered a threat. While shear-evaluating algorithms such as the tornado detection algorithm (TDA) (Mitchell et al. 1998) and mesocyclone detection algorithm (MDA) (Stumpf et al. 1998) are also available, meteorologists who are aggressively interrogating storms perform similar manual assessments rather than waiting for algorithm output which can shorten warning lead time. Manual evaluation of rotational shear over the depth of a storm is a labor-intensive and time-consuming process, and it is especially challenging when several storms require interrogation. Moreover, all three methods suffer from the inability to easily visualize spatial and temporal trends of mesocyclone or mesovortex evolution. Finally, these methods focus on single radar data unless forecasters can rapidly evaluate additional data from neighboring radar sites.

Since 2011, the NWS Davenport, Iowa office has informally evaluated several National Severe Storms Laboratory (NSSL) Multi-Radar Multi-Sensor (MRMS) products (Stumpf et al. 2003). The low-level rotation tracks product (Smith and Elmore 2004; Miller et al. 2013) generated particular interest because it provides a frequently updated (every two minutes) assessment of azimuthal shear that displays both a temporal and spatial history of the shear magnitude while utilizing data from all WSR-88D radars observing the storm in one product. Thus the rotation tracks product addresses many of the shortcomings of both manual methods for shear interrogation and the TDA and MDA algorithms.

With the operational deployment of a number of

* Corresponding author address: Raymond A. Wolf, NOAA/National Weather Service, 9050 Harrison St., Davenport, Iowa 52806; email: ray.wolf@noaa.gov

MRMS products in the NWS in 2015, an evaluation of the low-level rotation tracks was undertaken to encourage rapid adoption of the product into the warning decision making process with an understanding of its strengths and limitations.

2. DATA AND METHODS

Low-level (0-2 km) rotation tracks data with a spatial resolution of about 0.5 km from the NSSL On-demand System (2014) were compared to 186 observed tornadoes in Iowa between 2008 and 2014 (NCDC 2014). Iowa was selected as the area of study since the tornado climatology includes tornadoes generated by supercells, QLCSs, and non-supercell storms which permits evaluation of the rotation tracks in a variety of storm modes. The 186 tornadoes used for this study is a representative sample of the longer term EF-scale distribution (Fig. 1) (Cogil 2012). A large majority (85.5%) of tornadoes were rated EF0 and EF1. No EF5 tornadoes occurred during the period of study, although 1.6% were rated EF4. Most tornadoes were formally rated based on NWS storm surveys (53%). A myriad of other sources provided the initial tornado reports, most commonly trained spotters and emergency managers (Fig. 2).

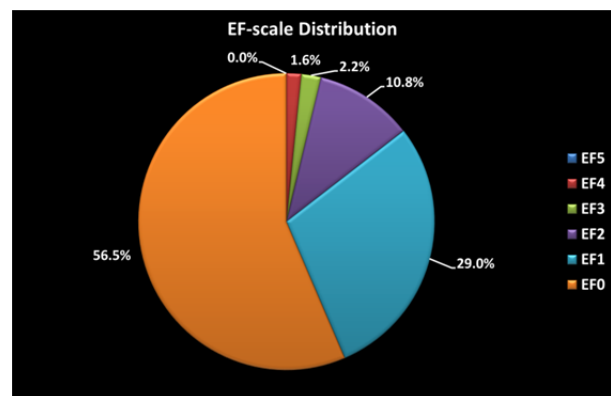


Figure 1. Distribution of EF-scale ratings for Iowa tornadoes, 2008-2014.

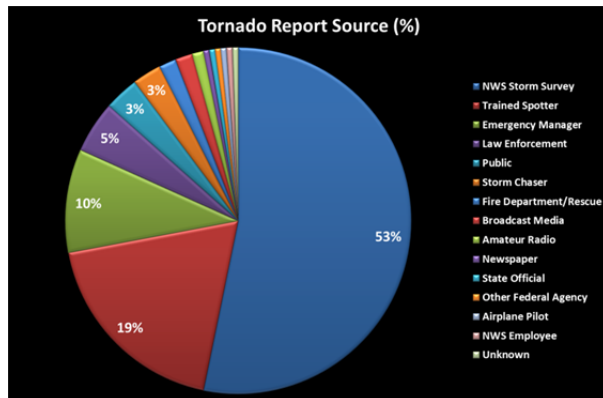


Figure 2. Sources of tornado reports in Iowa, 2008-2014.

Limitations of the NCDC tornado database are discussed by Doswell and Burgess (1988) and Grazulis (1993) who noted variances in the data due to population changes and reporting procedures. These points are likely not relevant to the short period of record used in this study since population was essentially static and reporting procedures unchanged. However, issues associated with population density biased reporting, plus challenges in determining F(EF)-scale ratings, do apply to the Iowa data set. In terms of evaluating the study findings, however, the main concern is the limited number of cold season tornadic events generated by supercells and QLCSs in the Iowa database. This could affect interpretation of the results when compared to areas where cold season events are a significant part of the local tornado climatology.

Azimuthal shear in the rotation tracks product was calculated using a Linear Least Squares Derivative algorithm (Smith and Elmore 2004) which removes much of the range dependency and has fewer false alarms compared to the MDA. Additional quality control techniques are employed to remove non-meteorological targets (Miller et al. 2013). Since rotation tracks are based on data from multiple radars, areas where undersampling occurs with one radar (e.g., due to range effects to beam height and width, cone of silence, terrain blockage, viewing angle) can be compensated for by the inclusion of data from neighboring radars.

The NSSL OnDemand database contained a few periods when one or more network radars were not available. These cases were removed from the study. Other database changes occurred during the period of study including improved techniques for calculating the tracks and WSR-88D network upgrades which increased base data resolution and added dual polarization capability. These improvements would logically have a positive influence on data quality.

While these database changes were not readily apparent in the final results, evaluating them was not a focus of this study.

Additional data quality issues include that shear calculations tend to break down within 5 km of a radar site which results in artificially-large values. These were easily identified and removed from the analysis. Smaller circulations may be underestimated in strength, though in contrast, larger circulations may be easier to identify in rotation tracks when compared to single radar base data. Finally, a reflectivity mask of 20 dBZ is used to filter circulations. Thus valid circulations could be removed as with a tornado associated with a very low reflectivity hook echo or a non-mesocyclone tornado (landspout) under a yet-to-be precipitating updraft column.

The following specific analyses were conducted:

- Assess the spatial relationship of the rotation track to the location of tornadogenesis.
- Evaluate the lead time from track initiation to tornadogenesis.
- Evaluate the relationship between shear magnitude and tornado EF-scale rating.
- Determine the shear distribution for observed tornadoes.

To assess the spatial relationship between the rotation track and location of tornadogenesis, the tornado was associated with the nearest shear maximum located at or immediately upstream of the tornado's initiation point. A five category classification was then employed as shown in figure 3. Tornadoes occurring within the core of the track (shear values $\sim .005 \text{ s}^{-1}$ and higher) were labeled IN, those on the fringe (shear values > 0 and $\sim < .005 \text{ s}^{-1}$) NEAR, those occurring approximately 10 minutes or less from the end of the track, END. These categories were considered hits for the algorithm. A miss for the algorithm was defined when a tornado occurred with no track at all or entirely outside of a nearby track.

The lead time between initiation of a rotation track and tornadogenesis was estimated by simply counting the number of shear maxima occurring in that time range and multiplying by 2, which is the product time interval in minutes (Fig. 4). The initiation of the rotation track is based on the first occurrence of a shear value of $.002 \text{ s}^{-1}$ or higher.

3. RESULTS AND DISCUSSION

The location of tornadogenesis was highly associated with the presence of a rotation track (Fig 5). Nearly 95% of the tornadoes studied initiated either

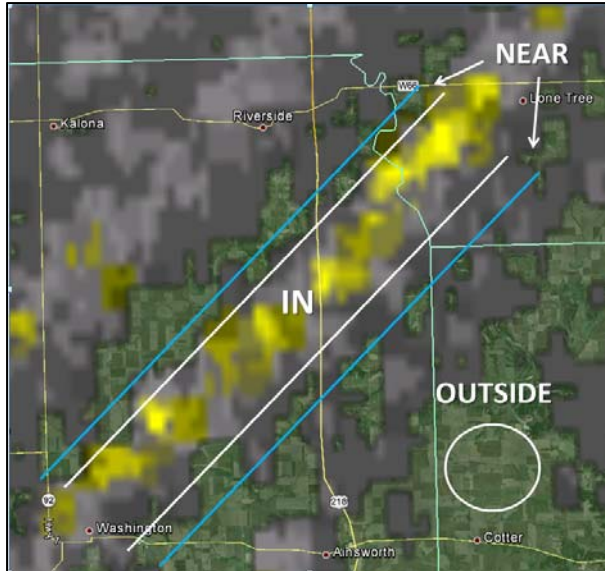


Figure 3. Spatial categorization of tornado initiation point relative to the rotation track. See text for details.

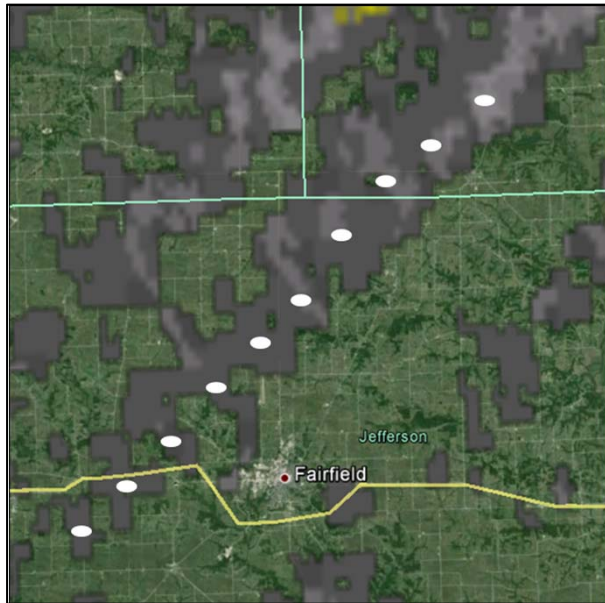


Figure 4. Estimated position of maxima is depicted by the white oval. Since each maximum occurs at the 2 minute product interval, these can be tallied to estimate the lead time between rotation track initiation and tornadogenesis.

within, near, or just after the end of a track. Less than 3% of cases occurred with no track, and less than 2% of cases occurred outside of a track. The latter may be associated with inaccurate tornado locations in the NCDC Storm Events database (Witt et al. 1998, Trapp et al. 2006). Based on review of the radar data for the four no-track tornadoes, it appears these cases were associated with weak, slow-moving convection, beyond 60 nm from the radar and thus could be landspouts. These type of tornadoes can be difficult to

observe even with single-radar velocity data, especially far from the radar (Brady and Szoke 1989).

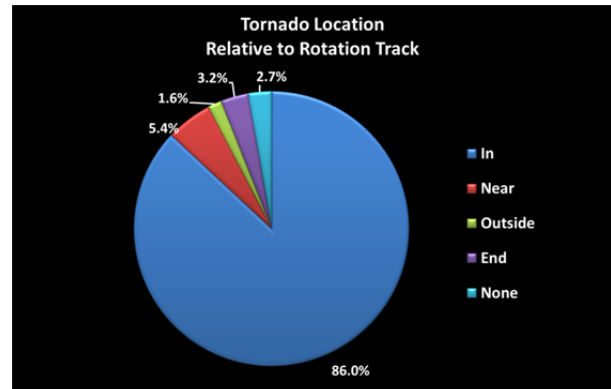


Figure 5. Frequency of tornadogenesis relative to rotation track location.

The time between inception of a rotation track and the subsequent tornado varied greatly from less than 5 minutes in numerous cases to more than 1 hour in a few cases (Fig. 6). The majority of cases had lead times around 20 minutes or less. Many of the longer lead times were associated with single tracks containing multiple tornadoes. The limited lead time between low-level mesocyclogenesis and tornadogenesis has been observed by Trapp et al. (1999), Kosiba et al. (2013), and others. These findings suggest that additional information such as mid-level rotation (tracks), environmental data, spotter observations, etc. is important when attempting to maximize tornado warning lead time.

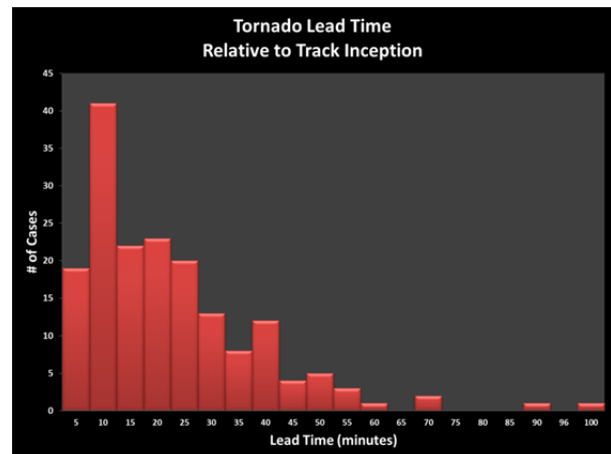


Figure 6. Lead time from inception of the rotation track to tornadogenesis.

The relationship between shear magnitude and EF-scale is not apparent in the data for EF0 and EF1 tornadoes, where cases were fairly evenly distributed

over a broad range of values (Fig. 7). There does appear to be a weak relationship within EF2-4 cases where stronger shear is associated with higher EF-scale ratings. However, there is much overlap between the EF0-1 and EF2-4 categories, so operational applications of these findings are limited. It is possible that increasing the number of cases with significant tornadoes may result a stronger relationship, so future efforts will investigate this assertion.

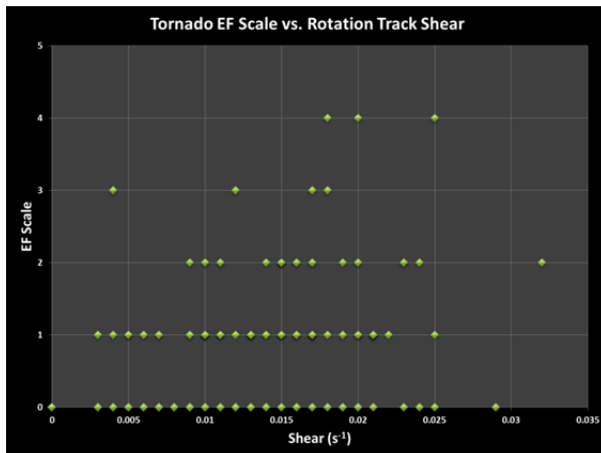


Figure 7. Relationship between tornado EF-scale rating and shear at or just before tornadogenesis.

Since the EF-scale is a damage-rating scale (Doswell and Burgess 1988), some of the variance observed may be attributed to the tornado not hitting a damage indicator of sufficient strength to justify a higher EF-scale rating. In addition, radar sampling issues can still be problematic with MRMS products if there is insufficient radar coverage to fully observe the circulation. This is the case in parts of southern and north central Iowa where the lowest WSR-88D network 0.5° beam centerline is 2-3 km above ground level.

The distribution of shear values for all tornadoes is shown in figure 8. This is the shear value occurring coincident with or immediately before the time of tornadogenesis. The standard box and whiskers diagram displays the median value ($.012 \text{ s}^{-1}$) as well as the 25th and 75th percentiles ($.017$ and $.008 \text{ s}^{-1}$ respectively), 90th and 10th percentiles ($.020$ and $.005 \text{ s}^{-1}$ respectively), and the range (0 to $.032 \text{ s}^{-1}$). Knowledge of these values provides forecasters a frame of reference for the magnitude of shear associated with tornadoes. It should be noted that similar to how not all mesocyclones in supercells nor all mesovortices in QLCSs produce tornadoes (Burgess et al. 1993, Trapp and Stumpf 2002, Atkins et al. 2004), not all rotation tracks are associated with tornadoes.

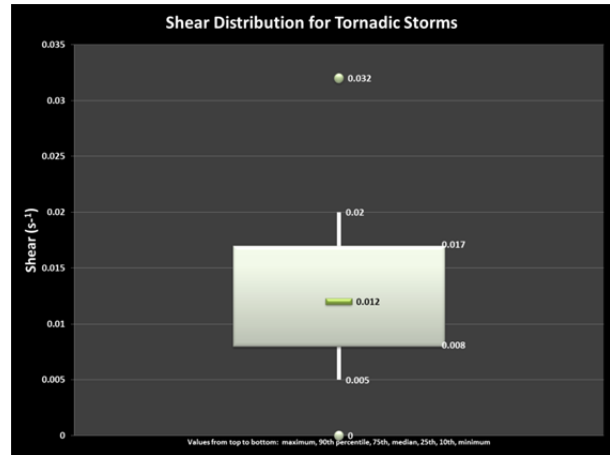


Figure 8. Shear distribution for all tornadoes at or just before tornadogenesis.

4. CONCLUSIONS

This study documents that tornadoes were nearly always associated with low-level rotation tracks during the period of study in Iowa. Exceptions include landspouts cases where velocity signatures are rarely observed, especially far from the radar. Most often tornadoes form within about 20 minutes of the inception of the rotation track, suggesting additional information regarding the mid-levels of the storm, environment, spotter observations, etc. need to be factored into the tornado warning decision making process to maximize lead time.

There is a weak relationship between shear value and EF scale for significant tornadoes (EF2+). But the relationship is too tenuous to be applied operationally without additional research since there is much overlap in shear values with EF0-1 tornadoes. The distribution of shear depicted in the box and whisker diagram (Fig. 8) should help forecasters develop a sense of the magnitude of shear values they can expect with a tornado. However, it should be emphasized that similar to supercells and QLCSs, not all circulations produce tornadoes, and not all rotation tracks are associated with tornadoes.

Operational experience has shown that with QLCSs, it is occasionally difficult to discriminate between shear associated with a mesovortex and shear along the gust front. Figure 9 shows a contrasting case of a supercell and QLCS track in the same image. The herring bone-like pattern created by the QLCS requires a more detailed evaluation for maxima reflecting the presence of a mesovortex versus the more straightforward appearance of the supercell's mesocyclone track. Evaluation of higher level scans from single radar data can help separate the deeper

mesovortex circulation from the shallower gust front shear zone. In cases like this, tornado lead time can be quite short regardless of the method of storm evaluation used in the warning process (Trapp et al. 1999). Training should insure that forecasters develop sufficient experience with the more complex QLCS rotation tracks signature versus the more straightforward supercell signatures.

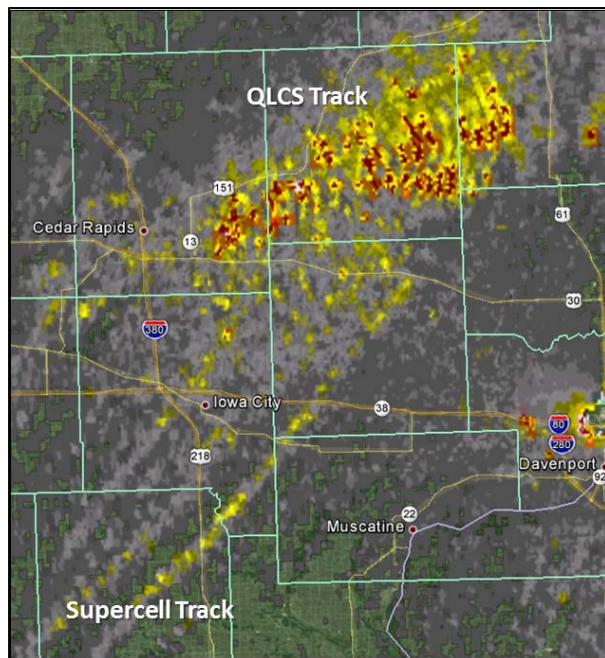


Figure 9. Rotation tracks associated with a supercell (lower left to center) and a QLCS (top). Note the herring bone-like appearance of the QLCS track versus the simple linear supercell track.

Operational experience also suggests rotation tracks in not a replacement for, but needs to be used in concert with single radar data analysis. Some circulations will appear slightly sooner and be better identified in single radar data, especially small circulations like those occurring with cold season events or at the leading edge of QLCSs. In contrast, very strong circulations are usually easier to identify in rotation tracks than with WSR-88D velocity products. Finally, training storms can be a challenge as newly developing storms track over and mask the track from prior storms.

5. REFERENCES

Atkins, N.T., J.M. Arnott, R.W. Pryzbylinski, R.W. Wolf, and B.D. Ketcham, 2004: Vortex structure and evolution within bow echoes. Part I: Single-Doppler

and damage analysis of the 29 June 1998 Derecho. *Mon. Wea. Rev.*, **132**, 2224-2242.

Brady, R.H., and E.J. Szoke, 1989: A case study of nonmesocyclone tornado development in northeast Colorado: Similarities to waterspout formation. *Mon. Wea. Rev.*, **117**, 843-856.

Burgess, D.W., R.J. Donaldson Jr., and P.R. Desrochers, 1993: *Tornado detection and warning by radar. The Tornado: Its Structure, Dynamics, Prediction and Hazards, Geophys. Monogr.*, No. 79, Amer. Geophys. Union, 203-221.

Cogil, C., 2012: Iowa tornado climatology 1980-2011. Unpublished report. [Available online at <http://www.crh.noaa.gov/Image/dmx/iowaTorClimatologyFinal-2011.pdf>].

Doswell, C. A., III, and D. W. Burgess, 1988: On some issues of United States tornado climatology. *Mon. Wea. Rev.*, **116**, 495-501.

Grazulis, T. P., 1993: Significant Tornadoes, 1680-1991. Environmental Films, 1326 pp.

Kosiba, K., J. Wurman, Y. Richardson, P. Markowski, P. Robinson, and J. Marquis, 2013: Genesis of the Goshen County, Wyoming, tornado on 5 June 2009 during VORTEX2. *Mon. Wea. Rev.*, **141**, 1157-1181,

Miller, M. L., V. Lakshmanan, and T. Smith, 2013: An Automated Method for Depicting Mesocyclone Paths and Intensities. *Wea. Forecasting*, **28**, 570-585.

Mitchell, E.D., S. V. Vasiloff, G. J. Stumpf, A. Witt, M. D. Eilts, J. T. Johnson, and K. W. Thomas, 1998: The National Severe Storms Laboratory tornado detection algorithm. *Wea. Forecasting*, **13**, 352-366.

NCDC, cited 2014: Storm Events Database. [Available online at <http://www.ncdc.noaa.gov/stormevents/>].

NSSL, cited 2014: WDSS-II OnDemand Database. [Available online at <http://ondemand.nssl.noaa.gov/>].

Smith, T., and K. L. Elmore, 2004: The use of radial velocity derivatives to diagnose rotation and divergence. Preprints, *11th Conf. on Aviation, Range, and Aerospace*, Hyannis, MA, Amer. Meteor. Soc., P5.6. [Available online at <http://ams.confex.com/ams/pdfpapers/81827.pdf>].

Stumpf, G. J., T. M. Smith, and C. Thomas, 2003: The National Severe Storms Laboratory's contribution to severe weather warning improvement: Multiple-sensor severe weather applications. *Atmos. Research*, **66**, 657-669.

Stumpf, G. J., A. Witt, E. D. Mitchell, P. L. Spencer, J. T. Johnson, M. D. Eilts, K. W. Thomas, and D. W. Burgess, 1998: The National Severe Storms Laboratory mesocyclone detection algorithm for the WSR-88D. *Wea. Forecasting*, **13**, 304-326.

Trapp, R.J., E.D. Mitchell, G.A. Tipton, D.W. Effertz, A.I. Watson, D.L. Andra, Jr., and M.A. Magsig, 1999: Descending and nondescending tornadic vortex signatures detected by WSR-88Ds. *Wea. Forecasting*, **14**, 625-639.

Trapp, R.J., and G.J. Stumpf, 2002: A reassessment of the percentage of tornadic mesocyclones. *Preprints, 21st Conf. on Severe Local Storms*, San Antonio, TX, Amer. Meteor. Soc., 198-201.

Trapp, R.J., D.M. Wheatley, N.T. Atkins, R.W. Przybylinski, and R. Wolf, 2006: Buyer beware: Some words of caution on the use of severe wind reports in postevent assessment and research. *Wea. Forecasting*, **21**, 408-415.

Witt, A., M.D. Eilts, G.J. Stumpf, E.D. Mitchell, J.T. Johnson, and K.W. Thomas, 1998: Evaluating the performance of WSR-88D severe storm detection algorithms. *Wea. Forecasting*, **13**, 513-518.